1 **Dietary protein source mediates colitis pathogenesis through bacterial modulation of bile**

2 **acids**

3   Simon M. Gray[1*], Michael C. Wood[2*], Samantha C. Mulkeen[2], Sunjida Ahmed[2], Shrey D.

4 Thaker[2], Bo Chen[2], William R. Sander[2], Vladimira Bibeva[2], Xiaoyue Zhang[3], Jie Yang[4], Jeremy

5 W. Herzog[1], Shiying Zhang[5], Belgin Dogan[5], Kenneth W. Simpson[5], R. Balfour Sartor[1,6,7] and

6 David C. Montrose[2,8]

7 [1]Center for Gastrointestinal Biology and Disease, Department of Medicine, University of North

8 Carolina, Chapel Hill, NC

9 [2]Department of Pathology, Renaissance School of Medicine, Stony Brook University, Stony

10 Brook, NY

11 [3]Biostatistical Consulting Core, Renaissance School of Medicine, Stony Brook University

12 [4]Department of Family, Population and Preventive Medicine, Stony Brook University, Stony

13 Brook, NY

14 [5]Department of Clinical Sciences, Cornell University, Ithaca, NY

15 [6]Department of Microbiology and Immunology, University of North Carolina, Chapel Hill, NC

16 [7]National Gnotobiotic Rodent Resource Center, University of North Carolina, Chapel Hill, NC

17 [8]Stony Brook Cancer Center, Stony Brook, NY.

18 ***Authors contributed equally.**

19 **Corresponding Author**: David C. Montrose, Department of Pathology, Renaissance School of

20 Medicine, Stony Brook University, MART Building, 9M-0816, Lauterbur Dr., Stony Brook, NY

21 11794. Phone: 631-216-2927; Fax: 631-444-3424; Email:

22 david.montrose@stonybrookmedicine.edu

30   **Declaration of interests:**

31   D.C.M. has consulting arrangements with Gleipnir Medical. The authors have no other

32   competing interests relevant to this study.

33   **Acknowledgements**

41

42   **Introductory paragraph**

43   Evidence-based dietary recommendations for individuals with inflammatory bowel

44   diseases (IBD) are limited. Red meat consumption is associated with increased IBD incidence

45   and relapse in patients, suggesting that switching to a plant-based diet may limit gut

46   inflammation. However, the mechanisms underlying the differential effects of these diets remain

47   poorly understood. Feeding diets containing plant- or animal-derived proteins to murine colitis

48   models revealed that mice given a beef protein (BP) diet exhibited the most severe colitis, while

49   mice fed pea protein (PP) developed mild inflammation. The colitis-promoting effects of BP were

50   microbially-mediated as determined by bacterial elimination or depletion and microbiota

51   transplant studies. In the absence of colitis, BP-feeding reduced abundance of *Lactobacillus*

52   *johnsonii* and *Turicibacter sanguinis* and expanded *Akkermansia muciniphila*, which localized to

2

53   the mucus in association with decreased mucus thickness and quality. BP-fed mice had

54   elevated primary and conjugated fecal bile acids (BAs), and taurocholic acid administration to

55   PP-fed mice worsened colitis. Dietary psyllium protected against BP-mediated inflammation,

56   restored BA-modulating commensals and normalized BA ratios. Collectively, these data suggest

57   that the protein component of red meat may be responsible, in part, for the colitis-promoting

58   effects of this food source and provide insight into dietary factors that may influence IBD

59   severity.

60

61   **Main Text**

62   Diet influences the pathogenesis and natural history of inflammatory bowel diseases

63   (IBD), disorders of chronic intestinal inflammation caused by dysregulated host immune

64   responses to resident intestinal microbes in genetically susceptible hosts[1-3]. Despite these

65   findings, limited evidence-based dietary recommendations exist to reduce the incidence and

66   severity of IBD[4-6]. For multiple decades IBD incidence has increased in the U.S. and globally,

67   including in regions with previously low rates[7-9]. Increased animal-based protein consumption,

68   including red meat, correlates with rising IBD incidence, suggesting a link between animal

69   protein consumption and IBD[10, 11]. However, the mechanisms by which specific dietary protein

70   sources promote gut inflammation remains unclear.

71   Diet regulates gut homeostasis and inflammation, in part, by shaping the composition,

72   function, and metabolic activity of the gut microbiota[2, 12-21]. For example, reducing dietary fiber or

73   increasing fructose consumption in mice enriches mucus-digesting resident bacteria, such as

74   *Akkermansia muciniphila*[12, 17-19, 21]. Further, consuming high fructose or dietary milk fat limits the

75   deconjugation of bile acids (BAs) (small molecules synthesized by the liver and modified by

76   intestinal microbes), resulting in increased levels of conjugated BAs (CBAs) and exacerbated

77   experimental colitis[17, 22]. Notably, patients with active IBD have higher levels of primary and

78   CBAs and depleted secondary unconjugated BAs, relative to healthy controls[23-25]. Moreover,

79 primary CBAs, which are metabolized by microbial enzymes to unconjugated secondary BAs,

80 exacerbate inflammation in experimental colitis models[22, 24, 26]. However, the role of dietary

81 protein source in these complex interactions and development of colonic inflammation is poorly

82 understood.

83   To investigate the impact of dietary protein source on experimental colitis severity, five

84 isocaloric synthetic diets containing protein isolates from beef, egg whites, casein, soy or pea

85 (**Table S1**) were fed to wild-type (WT) specific pathogen-free (SPF) C57BL/6J mice during

86 dextran sodium sulfate (DSS)-mediated induction of colitis. Mice fed beef protein (BP) diet

87 developed the most severe colitis while those fed pea protein (PP) diet developed the least

88 severe colitis; egg whites, casein, or soy protein diets induced intermediate colitis severity (**Fig.**

89 **1A-D**). BP feeding resulted in more severe colitis in a T-cell mediated colitis model using ex

90 germ-free (GF) $Il10^{-/-}$ mice colonized with mouse-adapted pooled human IBD microbiota (IMM-

91 HM2), to induce human IBD microbiota-associated colitis[27], compared to feeding a PP diet (**Fig.**

92 **1E-G**). This was characterized by greater weight loss, more severe histologic inflammation and

93 higher expression of colonic pro-inflammatory cytokines (**Fig. 1E-G**). Similar findings were made

94 in a second model of human IBD microbiota-associated colitis (IMM-g2)[27] (**Fig. 1H-J**). To

95 evaluate whether BP promotes colonic inflammation in the absence of a colitis inducer (i.e. DSS

96 or IBD patient-derived stool), WT SPF mice were fed standard chow, PP diet, or BP diet for 8

97 weeks and monitored, which showed no significant differences in DAI or colonic pro-

98 inflammatory cytokine expression (**Fig. S1A-B**). Collectively, these data demonstrate that the

99 protein component of beef worsens colonic inflammation in multiple experimental colitis models.

100   We next tested whether protein source modulates colitis severity, in part, through gut

101 resident bacteria. First, WT SPF mice were fed PP diet, BP diet, or BP diet in combination with

102 broad-spectrum antibiotics in drinking water to globally reduce gut bacteria, then challenged

103 with DSS while continuing the respective diets and antibiotics. Antibiotic treatment reduced BP

104 diet-mediated DSS colitis severity to, or below, PP diet-mediated levels (**Fig. 2A-C**). An ~500-

105   fold depletion in total bacterial abundance in feces of mice given antibiotics was confirmed by

106   qRT-PCR. Next, GF *Il10*^{-/-} mice were fed BP or PP diets for 14 days and assessed for colonic

107   inflammation by multiple parameters, which revealed no overt colitis in either group (**Fig. 2D-F**).

108   GF status in both groups was confirmed by anaerobic culture of feces (data not shown). Lastly,

109   we performed a fecal microbial transplant phenotype transfer experiment. Here, feces from WT

110   SPF mice fed BP or PP diets for 1 week were transplanted to GF WT mice fed standard rodent

111   chow and challenged with DSS for 10 days. Measurements of disease activity index (DAI),

112   colon length and histologic score showed that mice gavaged with fecal slurry from BP-fed mice

113   developed more severe colitis than mice administered feces from PP-fed mice (**Fig. 2G-I**).

114   Together, these data demonstrate that BP exacerbates colitis through the diet-altered

115   microbiota.

116   Since the dietary protein-altered microbiota mediates colitis severity, bacterial

117   community composition was profiled by 16S rRNA amplicon sequencing of feces from SPF WT

118   mice fed BP or PP diets for 1 week in the absence of colitis. Principal coordinates analysis

119   demonstrated distinct clustering of mice according to dietary protein source, which explained

120   approximately 65% of variation in the data (PERMANOVA test coefficient of determination, R^2 =

121   0.43, p=0.005) (**Fig 3A**). Although profiles before feeding either experimental diet were very

122   similar, 7 days of feeding BP or PP diet significantly altered the taxonomic abundance of

123   multiple bacteria (**Fig 3B; Fig. S2**). Significant expansion of *Akkermansia muciniphila* occurred

124   in the BP diet group, while *Turicibacter sanguinis* increased in the PP diet group, along with

125   preservation of *Lactobacillus johnsonii* (**Fig. 3B-C**). *A. muciniphila* can impair gut barrier function

126   through mucus digestion[12, 17, 21, 28-30], therefore, we examined its colonic luminal spatial

127   distribution by fluorescence *in situ* hybridization (FISH). This revealed high abundance of *A.*

128   *muciniphila* adjacent to the mucus layer of BP-fed mice while no signal was observed in PP-fed

129   mice (**Fig. 3D**). Colonic surface mucus thickness showed a corresponding ~50% reduction in

130   BP *vs*. PP fed mice (**Fig. 3E**). Additionally, surface mucus quality was reduced in BP- *vs*. PP-fed

131   mice with no obvious difference in goblet cell mucus staining (**Fig. 3F; Fig. S3**). To evaluate

132   whether BP-driven expansion of *A. muciniphila* was responsible, in part, for promoting colitis,

133   GF *Il10*^{-/-} mice were selectively colonized with *A. muciniphila* alone, a consortium of IBD-

134   associated pathobionts including *Escherichia coli*, *Enterococcus faecalis*, and *Ruminococcus*

135   *gnavus* (EER), or *A. muciniphila* plus EER and fed BP diet. Although *A. muciniphila* mono-

136   association did not induce colitis, it significantly potentiated EER pathobiont-induced colitis

137   severity (**Fig 3G-H**). Appropriate strain colonization was confirmed by anaerobic plating of feces

138   from colonized mice followed by 16S colony PCR and Sanger sequencing of representative

139   colony morphologies (data not shown). These data suggest that BP exacerbates colitis, in part,

140   by promoting expansion of mucus-digesting *A. muciniphila* that potentiates the pro-inflammatory

141   effects of IBD-associated pathobionts.

142   Because bacteria have an important role in mediating BA metabolism and composition

143   and there was higher abundance of bile salt hydrolase (BSH)-carrying[31-34] bacteria (*T sanguinis*,

144   *L johnsonii*) in PP-fed mice, we next measured the relative levels of common BAs in feces from

145   WT SPF mice fed BP or PP diets for 7 days in the absence of colitis. This analysis showed that

146   most BAs in BP-fed mice were primary and conjugated while most BAs in PP fed mice were

147   secondary and unconjugated (**Fig. 4A**). Multiple taurine conjugated primary BAs, including

148   taurocholic acid (TCA), were significantly higher in BP-fed mice while several unconjugated

149   secondary BAs, including lithocholic acid (LCA) and deoxycholic acid (DCA), were elevated in

150   PP-fed mice (**Fig. 4B**). These patterns were not observed in the livers or ileal content of mice

151   fed BP *vs*. PP diets (data not shown), suggesting that fecal BA alterations are likely mediated by

152   colon-specific microbial differences. To connect the respective BA profiles of mice fed PP or BP

153   diets with differential bacterial abundance, we performed an *in vitro* bile acid deconjugation

154   assay comparing select bacterial species enriched by either diet. This revealed that *L. johnsonii*

155   (higher abundance in PP-fed mice) deconjugated TCA to cholic acid (CA) 100-fold more than *A.*

156   *muciniphila* (increased in BP-fed mice) (**Fig. 4C**). To evaluate whether the primary CBAs that

157   were increased in feces of BP diet-fed mice directly exacerbate colitis, PP-fed mice were

158   administered TCA by oral gavage daily for 7 days and exposed to DSS. DAI, colon length and

159   histologic score showed that TCA worsened colitis in PP-fed mice (**Fig 4D-F**). Subsequent

160   MALDI-MSI based imaging of the colon of mice administered TCA in the absence of colitis

161   revealed TCA accumulation in the colonic epithelium (**Fig. S4**). Collectively, these data suggest

162   that mice consuming a BP-containing diet have lower abundance of BA-deconjugating bacteria,

163   resulting in higher levels of colitis-promoting primary CBAs.

164   Microbe-accessible dietary fiber supports populations of gut health-promoting

165   commensals, including BA-metabolizing bacteria[35]. Therefore, we reasoned that maintaining

166   these bacterial populations by adding soluble dietary fiber would attenuate BP-driven colitis

167   severity. To test this concept, ex-GF *Il10*$^{-/-}$ mice inoculated with MA human IBD microbiota were

168   fed PP diet, BP diet, or BP diet in which cellulose fiber was replaced with psyllium (BP-psyllium

169   diet) and monitored for colitis severity (**Table S1**). Compared to BP diet, the BP-psyllium diet

170   significantly decreased colitis severity, as determined by body weight, fecal lipocalin, histologic

171   analysis and cytokine gene expression (**Fig. 4G-J**). Similar protection by psyllium was observed

172   in the DSS-induced colitis model (**Fig. S5**). Analysis of BA-metabolizing bacteria and BA profiles

173   in WT C57BL/6J mice fed each of these three diets in the absence of colitis showed that

174   psyllium supplementation significantly increased the relative abundance of *L. johnsonii* and the

175   CA:TCA ratio in BP-fed mice (**Fig. 4K-L**). Taken together, these data support a model in which

176   BP-exacerbated colitis, which is driven by high abundance of primary CBAs, can be attenuated

177   through psyllium fiber administration, restoring populations of BSH-carrying bacteria that convert

178   primary CBAs to their deconjugated form.

179   Plant-based diets are believed to benefit IBD patients, while animal-based diets may be

180   detrimental. Both retrospective and prospective studies suggest that consumption of red meat is

181   associated with IBD incidence and disease activity. For example, The E3N Prospective Cohort

182   Study revealed that high animal protein consumption significantly increased IBD incidence[36] and

7

183   multiple studies showed that meat intake increased the risk of disease flare in patients with

184   ulcerative colitis (UC)[5, 37, 38]. The concept that plant-based diets are beneficial largely stems from

185   studies demonstrating that microbe-fermentable carbohydrates from plants reduce experimental

186   colitis[2, 39]. In contrast, diets rich in animal-derived products (especially red meat) are thought to

187   promote intestinal inflammation through heme, sulfur and saturated fat content[2, 39]. Although

188   these components of plant and animal-based diets impact gut health, the role of protein content

189   has not been widely considered. Our study, which selectively examined protein content by

190   feeding mice identical diets except for the type of protein isolate, suggests that the source of

191   dietary protein content differentially impacts colitis severity. Other studies investigating the

192   impact of protein source on experimental colitis, including from beef and pea, are largely

193   consistent with the data shown in the current study, although this previous work used diets

194   containing whole food sources rather than purified protein isolate[14, 15, 40, 41]. Our findings support

195   a role for the dietary protein-altered microbiota and BAs in mediating colitis severity, however,

196   the specific mechanism(s) by which protein type drives these effects remains unclear. It is

197   plausible that differences in amino acid composition or digestion/absorption of diverse dietary

198   protein sources are contributing factors. Therefore, determining which amino acids or what

199   properties of each protein type mediate intestinal inflammation will be important for future

200   studies.

201   Bacteria, BAs and their interplay are key mediators of IBD pathogenesis[1, 2]. Higher levels

202   of conjugated and primary BAs are found in feces of patients with active IBD, compared to

203   unconjugated and secondary BAs in healthy individuals[23-25]. Our work suggests that a shift to a

204   predominance of conjugated and primary BAs, is in part, responsible for greater colitis severity

205   when feeding BP to mice. We found that taurine conjugated and primary BAs are higher in BP-

206   fed mice than PP-fed mice, and showed that direct administration of TCA, which was highly

207   increased in the BP-fed group, worsened colitis in PP-fed mice to levels observed in mice given

208   BP diet alone. Although the exact mechanism(s) by which altered BAs enhance disease is

209 unclear, the detergent-like properties of BAs could disrupt gut barrier function by impairing

210 epithelial cell function and/or epithelial-protective mucus. This concept is supported by our data

211 showing the ability of exogenously administered TCA to localize to the colonic epithelium.

212 Interestingly, our prior work showed that a high fructose diet exacerbated murine colitis with a

213 similar increase in CBAs as observed in BP fed mice, with rectal administration of CBAs

214 worsening colitis and thinning colonic mucus in mice fed a control diet[17]. Integrating our study

215 focused on dietary protein with prior studies of the role of dietary fat and carbohydrates in

216 experimental colitis suggests that altered BAs may be a common pathway for diet-mediated gut

217 inflammation[17, 22]. Although our work focused on the detrimental impact of conjugated primary

218 bile acids enriched in BP-fed mice, the profile of unconjugated, secondary bile acids enriched in

219 feces from PP fed mice might itself be protective. For example, LCA and DCA, both enriched in

220 PP-fed mice, are strong ligands of the PXR and TGR5 receptors that, when activated, induce

221 anti-inflammatory effects[24, 42-44]. Therefore, the role of unconjugated secondary bile acids as

222 protective metabolites in PP-fed mice is an important future direction.

223   Bile acids have a bidirectional relationship with gut bacteria, whereby bacterial enzymes

224 metabolize BAs, which in turn, alter bacterial physiology and microbiota composition[42]. PP

225 feeding expanded bacterial species that efficiently deconjugate BAs, including *L johnsonii* and *T*

226 *sanguinis* (as shown by data from the deconjugation assay performed in the current study and

227 previous work[32]), while BP feeding expanded *A muciniphila,* a poor deconjugator that also

228 degrades mucus and potentiates pathobiont-driven inflammation[45]. These dietary protein-

229 induced bacterial shifts likely caused the observed BA profiles, however, we cannot exclude the

230 possibility that altered BAs directly shifted microbiota composition, as previously

231 demonstrated[46-49]. Further evidence that the ratio of conjugated to unconjugated BAs are

232 important for mediating colitis stems from our findings that psyllium supplementation protected

233 against BP-mediated colitis severity, while maintaining favorable BA profiles and populations of

234 BA-deconjugating bacteria. However, psyllium fiber likely protects against inflammation by

9

235   multiple mechanisms, including SCFA production and prevention of bacterial mucus

236   degradation[12, 50].

237   Our study reaffirms the concept that IBD occurs when multiple detrimental factors

238   intersect to initiate and perpetuate gut inflammation[51]. These IBD determinants – genetically

239   dysregulated host inflammatory and epithelial barrier responses, abnormal resident microbes,

240   and environmental triggers – can exist in isolation or combination without causing disease, but

241   together drive severe IBD. For example, GF colitis susceptible $Il10^{-/-}$ mice fed BP diet (genetic

242   susceptibility + environmental trigger) did not develop inflammation, nor did SPF WT mice fed

243   BP-diet (resident microbes + environmental trigger). However, we demonstrated that when all

244   three IBD-driving factors – host, microbe, and environment – intersect, severe and progressive

245   intestinal inflammation occurs. The poor long-term success of current human IBD therapies may

246   reflect a failure to reconcile the multiple determinants of IBD. For example, addressing just one

247   factor, such as suppression of host inflammation, leaves the patient vulnerable to recurrent

248   disease upon encountering environmental triggers. We suggest that durable long-term

249   remission requires simultaneously addressing all IBD determinants, and as such, investigations

250   into environmental drivers of IBD, especially diet, is required to guide clinical approaches to

251   maintain sustained remission.

252

253   **Methods**

254   *Murine colitis models*

255   To induce chemical colitis, 8-week-old male C57BL/6J mice (The Jackson Laboratory)

256   were administered 1% DSS (Sigma) in drinking water for 6–7 days, as indicated. Colitis severity

257   was assessed by measuring changes in body weight, as well as severity of rectal bleeding and

258   diarrhea, as previously described[17, 52]. Disease Activity Index (DAI) was calculated by combining

259   severity of body weight loss, diarrhea and bleeding, as previously described[17, 52].

260   T cell-mediated colitis was induced by inoculation of mouse-adapted human IBD patient

261   fecal microbiota (previously developed and characterized[27]) to GF $Il10^{-/-}$ mice on a 129S6/SvEv

262   background (purchased from the National Gnotobiotic Rodent Resource Center (NGRRC) at the

263   University of North Carolina), as previously described[27]. Mouse-adapted (MA) human IBD

264   patient microbiota was previously generated from de-identified human IBD patient stool samples

265   collected under an Institutional Review Board approved protocol; no primary human samples

266   were used in this study[27]. Briefly, human fecal materials from pooled cohorts of human donors

267   with active IBD were passaged through GF 129S6/SvEv $Il10^{-/-}$ mice to generate standardized

268   aliquots of fecal slurry[27]. MA IMM-g2 microbiota was derived from pooled feces of 2 CD and 1

269   UC patient and MA IMM-HM2 microbiota was derived from pooled feces of 3 CD patients[27].

270   Standardized 100mg/ml aliquots of mouse-adapted human IBD microbiota were anaerobically

271   thawed, diluted with pre-reduced PBS, and administered by oral gavage (2mg) to recipient GF

272    $Il10^{-/-}$ mice[27]. All fecal transplant experiments were performed with sterile gnotobiotic cage

273   technique in BSL-2 isolation cubicles with HEPA-filtered air[53]. Prior to colonization, GF mice

274   were fed Purina Advanced Protocol Select Rodent 50 IF/6F Auto Diet. Defined diets were

275   started at the time of fecal microbiota transplant.

276   At the end of the experimental periods, mice were humanely euthanized using CO_2.

277   Excised colons were measured then flushed with ice-cold phosphate-buffered saline (PBS).

278   Tissue was either snap-frozen for biochemical analysis or fixed in 4% paraformaldehyde or 10%

279   phosphate buffered formalin for 4-24 hours, followed by paraffin embedding and H&E staining

280   for histological analysis. All animal studies were approved by the Institutional Animal Care and

281   Use Committee at Stony Brook University and the University of North Carolina at Chapel Hill.

282

283   *Diet-polarized fecal microbiota transplant (FMT)*

284   Feces were collected from WT C57BL/6J SPF mice fed BP or PP diets for 2 weeks,

285   anaerobically homogenized, and diluted in pre-reduced lysogeny broth (LB) with 20% glycerol to

286   generate fecal slurries (n=5-6 donor mice per diet). Each donor FMT was administered to 1-2

287   recipient mice GF C57BL/6J mice via oral gavage on days 0, 3, 5, 7, and 9 of the experiment.

288   Mice were administered 2% DSS from days 3-10 of the experiment and monitored for signs of

289   colitis.

290

291   *Inoculation of defined consortia*

292   *Escherichia coli* LF82[54], *Enterococcus faecalis* OG1RF[55], and *Ruminococcus gnavus*

293   ATCC 29149[55] (EER) were grown under anaerobic conditions in brain-heart infusion medium

294   supplemented with 5g/L yeast extract, 0.5g/L L-cysteine, and 5mg/L hemin (LYH-BHI medium).

295   *A. muciniphila* ATCC BAA-835 (AM) was grown under anaerobic conditions in LYH-BHI medium

296   supplemented with 5g/L porcine gastric mucin (LYH-BHI + PGM). Pure cultures of each strain

297   were grown anaerobically to confluence then equally mixed to generate EER or EER + AM

298   consortia. GF 129S6/SvEv *Il10$^{-/-}$* mice were colonized with freshly cultured consortia by oral

299   gavage and given BP diet from the time of colonization. Feces were collected at necropsy, serial

300   diluted and plated under anaerobic conditions on LYH-BHI + PGM to confirm colonization with

301   consortia members. Representative colonies of each strain identified by colony morphology

302   were picked from plates, 16S PCR amplified, and Sanger sequenced (Eton Bioscience) to

303   confirm colonization of appropriate strains in recipient mice.

304

305   *Histopathologic scoring*

306   Colons from mice given DSS were flushed, formalin fixed, and paraffin embedded

307   followed by sectioning and staining with hematoxylin and eosin. Scoring of colitis/colonic

308   inflammation was performed based on evaluation of mucosal damage by acute inflammation, by

309   crypt abscess, mucosal architectural distortion and proportion of the involvement of colon as

310   previously described[56]. Briefly, epithelial damage by acute inflammation was graded into 4

311   categories (0-3; 0=no inflammation. 1=mild, 2=moderate and 3=severe inflammation with

12

312   ulceration). Mucosal damage with crypt abscess graded into 2 categories (0=absent and

313   1=present). Extent of acute inflammation was graded into 4 categories (0-3; 0=no inflammation,

314   1=mucosal, 2=submucosal and 3=transmural). Mucosal architectural distortion was graded into

315   4 categories which includes the percentage of length of colon involvement (0-3; 0=normal

316   architecture, 1= mild/focal or 10%, 2=moderate/20-30%, and 3=severe/ >40% of the entire

317   length). Proportion of the total involvement was evaluated by the percentage of length of colon

318   involved by colitis into 4 categories (0-3; 0=no colitis, 1=1-10% of the total length, 2=20-30%

319   and 3=>40% of the total evaluated length of colon). All histologic scoring was performed in a

320   blinded fashion by a board-certified gastrointestinal pathologist (S.A.).

321   For $Il10^{-/-}$ experimental colitis studies, histologic inflammation was quantified in ileal,

322   cecal and colonic (proximal, distal, rectal) tissue segments using a well-validated rubric by

323   blinded histopathology scoring on a scale of 0-4 for each segment, as previously described[27, 56,

324   57]. Total histology score was calculated by summation of all 5 tissue segment scores for a scale

325   of 0-20.

326

Fecal lipocalin-2 quantification

328   Fecal samples were homogenized in PBS with 0.1% Tween 20, incubated at 4°C for 12

329   hours, then centrifuged to yield clear supernatant for lipocalin-2 ELISA, performed according to

330   the manufacturer's instructions (DY1857, R&D Systems)[58].

331

Measurements of mucus thickness and quality

333   Segments of harvested colons from mice containing a fecal pellet were preserved in

334   fresh Carnoy's fixative solution (methanol:chloroform:glacial acetic acid, 60:30:10) then

335   sequentially washed in methanol, ethanol and xylenes, as previously described[17]. Tissues were

336   then paraffin-embedded and sectioned (5 μm), followed by staining with Alcian Blue, and mucus

337   thickness was measured in 20-50 regions of each colon in a blinded manner using ImageJ

338   software (National Institutes of Health, Bethesda, MD), as previously described[17].

339   To determine differences in mucus quality on the surface of the epithelium and within

340   goblet cells, Periodic acid Schiff (PAS) staining was performed. Stained slides were scanned

341   using an Aperio Image Scope (ScanScope, Aperio, CA) and used to count the PAS-positive

342   pixels by the Aperio Color Deconvolution algorithm, as previously described[17].

343

344   *qRT-PCR*

345   For measurements of mammalian gene expression, RNA was isolated from tissues

346   using QIAzol Lysis Reagent (Qiagen) following the manufacturer's protocol. RNA concentration

347   was measured using a NanoDrop ND-1000 spectrophotometer. cDNA was synthesized using

348   2000 ng total RNA and reverse transcriptase qScript SuperMix (Quanta). Quantitative real-time

349   PCR was performed using specific primers on a QuantStudio 7 Real-Time PCR System

350   (Applied Biosystems) using PowerTrack SYBR Green PCR Master Mix and oligo (dT) primers

351   according to the user's manual. *Actb* expression was used as internal control for gene

352   expression. The ΔΔCT method was used to calculate relative fold expression. Primer

353   sequences are shown in **Table S2**.

354   For bacterial abundance and bacterial gene expression analysis, DNA was extracted

355   from fecal samples using the QIAamp DNA Fast Stool Mini Kit (Qiagen) per the manufacturer's

356   instructions. For each sample, 10 ng of DNA was used for qRT-PCR using PowerTrack SYBR

357   green PCR master mix on a QuantStudio 7 PCR Machine. Bacterial primers sequences are

358   shown in **Table S2**. Relative abundance was calculated by the ΔΔCT method using universal

359   16S primers as control.

360

361   *Bile acid analysis*

362   Fecal and ileal samples were dried in a vacuum centrifuge then homogenized in 500 µL

14

363   of cold 80% methanol. Liver samples were homogenized using the same method but without

364   prior drying. Bacterial supernatants were mixed with cold 80% methanol in a 1:9 ratio. Following

365   homogenization or mixing, samples were centrifuged at 14,000 rcf for 20 minutes at 4°C and the

366   supernatant was collected and dried down using a vacuum centrifuge then stored at -80° C prior

367   to analysis. Bile Acid analysis was performed as previously described on a Vanquish UHPLC

368   system coupled to a Q Exactive Orbitrap mass spectrometer (Thermo Scientific)[17].

369   Relative quantitation was normalized to dry weight of fecal/ileal samples or protein

370   concentration of livers. Analysis was performed at the Proteomics & Metabolomics Core Facility

371   of Weill Cornell Medicine.

372

373   *MALDI Mass Spectrometry Imaging*

374   Tissue preparation and imaging was performed following a previously published

375   method[59]. Briefly, mouse colons were processed into Swiss-rolls, embedded in 5%

376   carboxymethylcellulose, and stored at -20°C. Serial frozen sectioning was performed for paired

377   MALDI imaging and standard H&E staining. MALDI imaging was conducted on a rapifleX mass

378   spectrometer (Bruker Daltonics) within metabolite mass range in negative ion detect mode at 50

379   µm spatial resolution. The TCA deprotonated ion with a mass-to-charge ratio of 514.284 m/z

380   was detected, and the average intensity of the mass spectrometry signal for TCA determined

381   using SCiLS Lab software (Bruker Daltronics).

382

383   *16S rRNA Analysis*

384   Frozen fecal samples were shipped to Molecular Research (Shallowater, TX) for 16S

385   rRNA profiling, performed as previously described[17]. DNA was extracted with the Powersoil

386   DNA Kit (Qiagen). The 16S rRNA gene V4 variable region was targeted for PCR amplification,

387   followed by Illumina HiSeq short-read sequencing. Sequencing outputs were processed and

388   taxonomically classified as previously described[17]. Operational taxonomic units were defined by

389   clustering at 97% similarity (3% divergence) and classified by BLASTn against an RDPII/NCBI

390   derived database. Statistical analysis and visualization of principal coordinates analysis (PCoA)

391   plots were performed with the Shiny application *Plotmicrobiome* (Sun et al. GitHub

392   https://github.com/ssun6/plotmicrobiome).

393

394   *Fluorescence in situ hybridization (FISH)*

395   Fluorescence in situ hybridization (FISH) was performed as previously described[17, 60] on

396   4μm histologic sections of Carnoy's-fixed paraffin-embedded colon tissue using an *A.*

397   *muciniphila*-specific FISH probe (S-SMUC-1437-a-A-20: Cy-3-50-

398   CCTTGCGGTTGGCTTCAGAT-30)[17, 60]. Slides spotted with multiple control bacteria (*E. coli, P*

399   *vulgaris, K pneumoniae, S equi, S bovis*) not-reactive to the A.M. FISH probe were used to

400   confirm probe specificity[17, 60].

401

402   *In vitro bacterial culture and treatment*

403   *L. johnsonii* BAA-3147 and *A. muciniphila* BAA-835 from frozen stocks were cultured

404   overnight in MRS or LYH-BHI + 0.5% mucin, respectively, the day before the experiments. *A.*

405   *muciniphila* BAA-835 was cultured in an anaerobic chamber (Coy Laboratory) with mixed gas

406   (90% N2, 5% CO2 and 5% H2; 37°C), and *L. johnsonii* BAA-3147 was cultured under aerobic

407   conditions (37°C with shaking at 150 rpm). The overnight cultures were diluted with fresh media

408   with or without 1 mM taurocholate to *A. muciniphilla* BAA-835 (once at OD600 of 1-1.1) and to

409   *L. johnsonii* (once at OD600 of 0.7-0.8). The diluted cultures were immediately distributed into

410   two sets of tubes for 0 and 24 h time points, each in triplicate. The time 0 h samples were

411   transferred to ice immediately to prevent bacterial activity on taurocholate. Optical densities

412   were measured at each time point for normalization. The cultures were then centrifuged at

413   3,000 rpm for 20 min at 4°C and the supernatants were filtered through a 0.2 μm syringe filter

414   and kept at -80°C until BA measurements.

415

Statistical analysis

417   For the comparison of DAI across different mice groups, linear mixed-effects models for

418   longitudinal data analysis were used. Model assumption was confirmed using residual

419   diagnosis. Time (in days) was treated as a continuous variable to assess the trend in DAI. An

420   interaction term between diet group and time was used to compare the trends across groups.

421   The covariance structure used to model the correlated longitudinal measurements from the

422   same mice was unstructured (UN), selected based on Akaike Information Criterion (AIC) from a

423   set of possible structures. For the comparison of numeric values observed or calculated at the

424   end of experiments, Wilcoxon rank-sum tests or simple linear regression models were used.

425   These analyses were applied to the following variables: % body weight change, histology score,

426   gene expression, colon length, bacterial abundance, mucus thickness, mucus quality, and bile

427   acid ratios. A P-value less than 0.05 was considered statistically significant and analyses were

428   performed using SAS 9.4 (SAS Institute Inc., Cary, NC).

429   <u>Statistical analysis of BA levels.</u> The BA dataset was filtered to remove BA with >50%

430   missing values. Normalization of raw metabolite levels was performed by probabilistic quotient

431   normalization followed by log2-transformation and imputation of missing values by k-nearest

432   neighbor (KNN). BA differences were quantified by log2 fold change from the PP diet group.

433   Linear models with diet as the independent variable were used to calculate statistical

434   significance. The Benjamini-Hochberg method with an FDR cut-off of 0.2 was used for multiple

435   hypothesis correction. Analyses were performed with the maplet package (version 1.2.1) in R [61].

436

437   **Figure Legends**

438   **Figure 1. Dietary beef protein worsens murine colitis compared to other protein sources**

439   A-D, C57BL/6 mice were fed isocaloric diets containing protein isolate derived from beef (BP),

440   soy (SP), egg whites (EP), casein (CP), or pea (PP) for 7 days, followed by administration of 1%

441   DSS for 7 days, while being continued on the respective diets. Disease activity index (DAI) was

442   measured during DSS exposure (A), percent of body weight change relative to day 0 of DSS

443   exposure was calculated following 7 days of DSS administration (B) and histologic score was

444   assessed in colons on day 7 of DSS administration (C). n = 6 mice per group. Representative

445   histologic images of colons from BP or PP-fed mice are shown (D). E-G, germ-free $Il10^{-/-}$ mice

446   were inoculated with mouse-adapted (MA) pooled human IBD patient fecal microbiota (IMM-

447   HM2) then fed diets containing BP or PP for 14 days. Weight change relative to day 0 was

448   measured (E), representative histologic images of colons are shown (left side) and total

449   histology score was assessed (right side) (F), and relative gene expression of cytokines were

450   measured in colons (G), on day 14. n = 7-8 mice per group. H-J, germ-free $Il10^{-/-}$ mice were

451   inoculated with a second MA pooled human IBD patient fecal microbiota (IMM-g2) then fed BP

452   or PP diets for 8 days. Weight changes relative to day 0 were measured (H), representative

453   histologic images of colons are shown (left side) and rectal histology score was assessed (right

454   side) (I), and relative gene expression of cytokines were measured in colons (J), on day 8. n =

455   4-6 mice per group. Data representative of 3 (E-G), and 3 (H-J) independent experiments.

456   *P<0.05; **P<0.01; ***P<0.001; ****P<0.0001. Bar plots show mean and standard deviation.

457

458   **Figure 2. Gut bacteria are causally linked to beef protein-worsening of colitis**

459   A-C, C57BL/6J mice were fed beef protein (BP) or pea protein (PP)-containing diets or beef

460   protein diet and administered a five-antibiotic cocktail (ampicillin, gentamicin, metronidazole,

461   neomycin, vancomycin[17]) in drinking water for 14 days (BP + Abx), then all mice were given 1%

462   DSS in drinking water for 7 days while being continued on control or antibiotics-containing

463   water. Disease Activity Index (DAI) was measured during DSS exposure (A), colon length was

464   measured on day 7 (B) and histologic inflammation of colons was assessed on day 7 (C). n = 8

465   mice per group. D-F, germ-free $Il10^{-/-}$ mice were fed sterile BP or PP diets for 14 days.

466   Representative histologic images of colons are shown (D), histology score was assessed (E)

467 and relative gene expression of *Il1b* was measured in colons (F), on day 14. n = 4-5 mice per

468 group. G-I, germ-free wild-type mice were inoculated with colonic luminal fecal contents of

469 specific pathogen-free mice fed BP or PP diets for 7 days. Recipient mice were then fed

470 standard chow and administered 1% DSS for 7 days and DAI was calculated (G), colon length

471 was measured (H) and histologic inflammation of colons was assessed (I), on day 10. n = 9-10

472 per group; data are representative of 2 independent experiments. *P<0.05; **P<0.01;

473 ***P<0.001; ****P<0.0001. Bar plots show mean and standard deviation.

474

475 **Figure 3. Beef protein consumption promotes *A. muciniphila* expansion and gut barrier**

476 **defects**

477 A-C, C57BL/6J mice were fed either beef protein (BP) or pea protein (PP)-containing diets for 7

478 days then fecal samples were subjected to 16S rRNA sequencing. Results are displayed as

479 principal coordinate analysis on day 7 (A) and as percent abundance of each species on days 0

480 and 7 (B) (those species <1% in overall abundance are labeled as 'Other'). qRT-PCR was

481 performed on fecal DNA to measure relative abundance of major populations found in either diet

482 group (C). D-F, C57BL/6J wild-type mice were fed BP or PP diets for 7 days then colons were

483 harvested and fixed to preserve the mucus layer. Fluorescence *in situ* hybridization was

484 performed to identify *A. muciniphila* (indicated by orange structures) (D), Alcian blue staining

485 was carried out to measure mucus thickness (representative images shown on left side and

486 quantification of staining shown on right side; bracket indicates mucus layer on images) (E), and

487 periodic acid Schiff staining was performed to quantify mucus quality (representative images

488 shown on left side and quantification of staining shown on right side) (F). n = 6 per group. G-H,

489 germ-free *Il10*$^{-/-}$ mice were inoculated with *A. muciniphila*, a defined consortium of *Escherichia*

490 *coli*, *Enterococcus faecalis*, and *Ruminococcus gnavus* alone or in combination with *A.*

491 *muciniphila* and fed BP diet. Representative histologic images of ceca are shown (left side) and

492 total histology score was assessed (right side) (G) and relative expression of inflammatory

493   cytokine genes was measured (H) in the ceca of mice on day 14. n = 7-9 per group, data

494   representative of 2 independent experiments. *P<0.05; **P<0.01; ***P<0.001; ****P<0.0001. Bar

495   plots show mean and standard deviation.

496

497   **Figure 4. Bacteria-mediated bile acid changes facilitate colitis severity**

498   A-B, WT C57BL/6J mice were fed diets containing either beef protein (BP) or pea protein (PP)-

499   containing diets for 7 days and the relative abundance of bile acids was measured in feces. The

500   average percent of primary *vs*. secondary or conjugated *vs*. unconjugated bile acids in each diet

501   group is shown (A) and those BAs that displayed significantly different abundance (FDR<0.1)

502   are shown as log2 fold-change in PP-fed mice relative to BP-fed mice (B). C, taurocholic acid

503   (TCA) (1mM) was administered to culture medium of *L. johnsonii* and *A. muciniphila* and the

504   levels of cholic acid were measured in the supernatants after 24 hours and reported as relative

505   to either species cultured in the absence of TCA. D-F, C57BL/6J WT mice were fed either BP or

506   PP diets and given daily oral gavage of PBS or fed PP and gavaged daily with TCA (0.35mg/kg)

507   for 7 days, then administered 1% DSS in drinking water for 7 days, while continuing oral

508   administration. Disease Activity Index (DAI) was measured over 7 days (D), colon length was

509   measured on day 7 (E) and histologic inflammation of colons was assessed on day 7 (F). G-J,

510   germ-free $Il10^{-/-}$ mice were inoculated with mouse-adapted pooled human IBD patient fecal

511   microbiota (IMM-HM2) then fed BP or PP diets containing cellulose or BP diet containing

512   psyllium (BP + psyllium) for 14 days. Weight changes relative to day 0 were calculated (G),

513   fecal lipocalin-2 (f-Lcn) was measured (H), total histology score was assessed (I), and relative

514   gene expression of inflammatory cytokines in colons was measured (J), on day 14. n = 10-11

515   mice per group. K-L, WT specific pathogen-free mice were fed the diets described in panel G for

516   7 days and feces were collected to measure the relative abundance of *L. johnsonii* by qRT-PCR

517   (K) and the ratio of cholic acid to taurocholic acid (CA:TCA) in fecal samples (L). n = 10-11 mice

518   per group. *P<0.05; **P<0.01; ***P<0.001; ****P<0.0001. Bar plots show mean and standard

519   deviation.

520

521   **Supplementary Figure Legends**

522   **Figure S1**. **Long-term beef protein feeding in specific pathogen free wild-type mice does**

523   **not induce signs of colitis.** Mice were fed chow, or purified diet containing beef protein (BP) or

524   pea protein (PP) isolate for 8 weeks. Disease activity index (DAI) was measured weekly (A) and

525   relative expression of *Tnfa* and *Il1b* was measured in colons at the end of the study (B). n = 6

526   mice per group. Bar plots show mean and standard deviation.

527

528   **Figure S2**. **Relative bacterial species abundance of individual mice fed beef or pea**

529   **protein-containing diets.** Species abundance in feces from individual mice is reported prior to

530   (A) and 7 days following (B) administration of diets containing beef protein (BP) or pea protein

531   (PP) isolate. Those species appearing in abundance <1% in all conditions are labeled as

532   'Other'.

533

534   **Figure S3. Dietary protein source does not affect goblet cell mucus quality.** C57BL/6J

535   mice were fed either beef protein (BP) or pea protein (PP)-containing diets for 7 days then

536   periodic acid Schiff staining was performed to quantify mucus quality within goblet cells.

537   Representative images (A) and quantification of staining (B) are shown. Bar plots show mean

538   and standard deviation.

539

540   **Figure S4**. **Taurocholic acid localizes to the colonic epithelium following oral**

541   **administration to mice.** C57BL/6J WT mice were administered daily oral gavage of PBS or

542   taurocholic acid (TCA) (0.35mg/kg) for 7 days and colon tissue sections were subjected to

543   MALDI-MSI to determine localization (A) and relative abundance (B) of TCA in each group. TCA

21

544   group is normalized to vehicle group in panel B. n = 4 samples per group. **P<0.01. Bar plots

545   show mean and standard deviation.

546

547   **Figure S5**. **Psyllium supplementation protects against beef protein diet-induced**

548   **worsening of DSS-induced colitis.** WT specific pathogen free mice were fed beef protein (BP)

549   or pea protein (BP) diets containing cellulose or BP diet containing psyllium (BP + Psyllium) for

550   7 days. Mice were then administered 1% dextran sodium sulfate (DSS) and Disease Activity

551   Index (DAI) was measured over 7 days (A) and colon length was measured on day 7 (B). Bar

552   plots show mean and standard deviation.

553

554   **References**

555
556   1.   Sartor RB, Wu GD. Roles for Intestinal Bacteria, Viruses, and Fungi in Pathogenesis of
557   Inflammatory Bowel Diseases and Therapeutic Approaches. Gastroenterology.
558   2017;152(2):327-39.e4.
559   2.   Perler BK, Friedman ES, Wu GD. The role of the gut microbiota in the relationship
560   between diet and human health. Annual review of physiology. 2023;85:449-68.
561   3.   Lee D, Albenberg L, Compher C, Baldassano R, Piccoli D, Lewis JD, et al. Diet in the
562   Pathogenesis and Treatment of Inflammatory Bowel Diseases. Gastroenterology.
563   2015;148(6):1087-106.
564   4.   Gleave A, Shah A, Tahir U, Blom J-J, Dong E, Patel A, et al. Using Diet to Treat
565   Inflammatory Bowel Disease: A Systematic Review. Official journal of the American College of
566   Gastroenterology | ACG. 2025;120(1).
567   5.   Issokson K, Lee DY, Yarur AJ, Lewis JD, Suskind DL. The Role of Diet in Inflammatory
568   Bowel Disease Onset, Disease Management, and Surgical Optimization. Official journal of the
569   American College of Gastroenterology | ACG. 2025;120(1).
570   6.   Hashash JG, Elkins J, Lewis JD, Binion DG. AGA Clinical Practice Update on Diet and
571   Nutritional Therapies in Patients With Inflammatory Bowel Disease: Expert Review.
572   Gastroenterology. 2024;166(3):521-32.
573   7.   Kaplan GG, Ng SC. Understanding and Preventing the Global Increase of Inflammatory
574   Bowel Disease. Gastroenterology. 2017;152(2):313-21.e2.
575   8.   Kaplan GG, Windsor JW. The four epidemiological stages in the global evolution of
576   inflammatory bowel disease. Nature Reviews Gastroenterology & Hepatology. 2021;18(1):56-
577   66.
578   9.   Kuenzig ME, Fung SG, Marderfeld L, Mak JWY, Kaplan GG, Ng SC, et al. Twenty-first
579   Century Trends in the Global Epidemiology of Pediatric-Onset Inflammatory Bowel Disease:
580   Systematic Review. Gastroenterology. 2022;162(4):1147-59.e4.
581   10.   Daniel CR, Cross AJ, Koebnick C, Sinha R. Trends in meat consumption in the USA.
582   Public Health Nutrition. 2011;14(4):575-83.

583   11.   Al Hasan SM, Saulam J, Mikami F, Kanda K, Ngatu NR, Yokoi H, et al. Trends in per
584   Capita Food and Protein Availability at the National Level of the Southeast Asian Countries: An
585   Analysis of the FAO's Food Balance Sheet Data from 1961 to 2018. Nutrients. 2022;14(3).
586   12.   Desai MS, Seekatz AM, Koropatkin NM, Kamada N, Hickey CA, Wolter M, et al. A
587   Dietary Fiber-Deprived Gut Microbiota Degrades the Colonic Mucus Barrier and Enhances
588   Pathogen Susceptibility. Cell. 2016;167(5):1339-53.e21.
589   13.   Hryckowian AJ, Van Treuren W, Smits SA, Davis NM, Gardner JO, Bouley DM, et al.
590   Microbiota-accessible carbohydrates suppress Clostridium difficile infection in a murine model.
591   Nature Microbiology. 2018;3(6):662-9.
592   14.   Llewellyn SR, Britton GJ, Contijoch EJ, Vennaro OH, Mortha A, Colombel J-F, et al.
593   Interactions Between Diet and the Intestinal Microbiota Alter Intestinal Permeability and Colitis
594   Severity in Mice. Gastroenterology. 2018;154(4):1037-46.e2.
595   15.   Kostovcikova K, Coufal S, Galanova N, Fajstova A, Hudcovic T, Kostovcik M, et al. Diet
596   Rich in Animal Protein Promotes Pro-inflammatory Macrophage Response and Exacerbates
597   Colitis in Mice. Front Immunol. 2019;10.
598   16.   Riva A, Kuzyk O, Forsberg E, Siuzdak G, Pfann C, Herbold C, et al. A fiber-deprived diet
599   disturbs the fine-scale spatial architecture of the murine colon microbiome. Nature
600   Communications. 2019;10(1):4366.
601   17.   Montrose DC, Nishiguchi R, Basu S, Staab HA, Zhou XK, Wang H, et al. Dietary
602   Fructose Alters the Composition, Localization, and Metabolism of Gut Microbiota in Association
603   With Worsening Colitis. Cellular and Molecular Gastroenterology and Hepatology.
604   2021;11(2):525-50.
605   18.   Neumann M, Steimle A, Grant ET, Wolter M, Parrish A, Willieme S, et al. Deprivation of
606   dietary fiber in specific-pathogen-free mice promotes susceptibility to the intestinal mucosal
607   pathogen Citrobacter rodentium. Gut Microbes. 2021;13(1):1966263.
608   19.   Wolter M, Steimle A, Parrish A, Zimmer J, Desai Mahesh S. Dietary Modulation Alters
609   Susceptibility to Listeria monocytogenes and Salmonella Typhimurium with or without a Gut
610   Microbiota. mSystems. 2021;6(6):e00717-21.
611   20.   Shan Y, Lee M, Chang EB. The Gut Microbiome and Inflammatory Bowel Diseases.
612   Annu Rev Med 2022;73:455-468.
613   21.   Pereira GV, Boudaud M, Wolter M, Alexander C, De Sciscio A, Grant ET, et al.
614   Opposing diet, microbiome, and metabolite mechanisms regulate inflammatory bowel disease in
615   a genetically susceptible host. Cell Host & Microbe. 2024;32(4):527-42.e9.
616   22.   Devkota S, Wang Y, Musch MW, Leone V, Fehlner-Peach H, Nadimpalli A, et al.
617   Dietary-fat-induced taurocholic acid promotes pathobiont expansion and colitis in Il10-/- mice.
618   Nature. 2012;487(7405):104-8.
619   23.   Lloyd-Price J, Arze C, Ananthakrishnan AN, Schirmer M, Avila-Pacheco J, Poon TW, et
620   al. Multi-omics of the gut microbial ecosystem in inflammatory bowel diseases. Nature.
621   2019;569(7758):655-62.
622   24.   Sinha SR, Haileselassie Y, Nguyen LP, Tropini C, Wang M, Becker LS, et al. Dysbiosis-
623   Induced Secondary Bile Acid Deficiency Promotes Intestinal Inflammation. Cell Host & Microbe.
624   2020;27(4):659-70.e5.
625   25.   Yang ZH, Liu F, Zhu XR, Suo FY, Jia ZJ, Yao SK. Altered profiles of fecal bile acids
626   correlate with gut microbiota and inflammatory responses in patients with ulcerative colitis.
627   World J Gastroenterol. 2021:June 28;7(4):3609-29.
628   26.   Joyce SA, Gahan CGM. Bile Acid Modifications at the Microbe-Host Interface: Potential
629   for Nutraceutical and Pharmaceutical Interventions in Host Health. Annual review of food
630   science and technology. 2016;7(1):313-33.
631   27.   Gray SM, Moss AD, Herzog JW, Kashiwagi S, Liu B, Young JB, et al. Mouse adaptation
632   of human inflammatory bowel diseases microbiota enhances colonization efficiency and alters

microbiome aggressiveness depending on the recipient colonic inflammatory environment. Microbiome. 2024;12(1):147.

28. Png CW, Lindén SK, Gilshenan KS, Zoetendal EG, McSweeney CS, Sly LI, et al. Mucolytic Bacteria With Increased Prevalence in IBD Mucosa AugmentIn VitroUtilization of Mucin by Other Bacteria. Official journal of the American College of Gastroenterology | ACG. 2010;105(11).

29. Seregin SS, Golovchenko N, Schaf B, Chen J, Pudlo NA, Mitchell J, et al. NLRP6 Protects Il10-/- Mice from Colitis by Limiting Colonization of Akkermansia muciniphila. Cell Reports. 2017;19(4):733-45.

30. Sugihara K, Kitamoto S, Saraithong P, Nagao-Kitamoto H, Hoostal M, McCarthy C, et al. Mucolytic bacteria license pathobionts to acquire host-derived nutrients during dietary nutrient restriction. Cell Reports. 2022;40(3).

31. Hoek Kristen L, McClanahan Kathleen G, Latour Yvonne L, Shealy N, Piazuelo MB, Vallance Bruce A, et al. Turicibacterales protect mice from severe Citrobacter rodentium infection. Infect Immun. 2023;91(11):e00322-23.

32. Lynch JB, Gonzalez EL, Choy K, Faull KF, Jewell T, Arellano A, et al. Gut microbiota Turicibacter strains differentially modify bile acids and host lipids. Nature Communications. 2023;14(1):3669.

33. Zhang W, Wang J, Zhang D, Liu H, Wang S, Wang Y, et al. Complete Genome Sequencing and Comparative Genome Characterization of Lactobacillus johnsonii ZLJ010, a Potential Probiotic With Health-Promoting Properties. Frontiers in Genetics. 2019;10.

34. Jia D-J-C, Wang Q-W, Hu Y-Y, He J-M, Ge Q-W, Qi Y-D, et al. Lactobacillus johnsonii alleviates colitis by TLR1/2-STAT3 mediated CD206+ macrophagesIL-10 activation. Gut Microbes. 2022;14(1):2145843.

35. Kastl A, Zong W, Gershuni VM, Friedman ES, Tanes C, Boateng A, et al. Dietary fiber-based regulation of bile salt hydrolase activity in the gut microbiota and its relevance to human disease. Gut Microbes. 2022;14(1):2083417.

36. Jantchou P, Morois S, Clavel-Chapelon F, Boutron-Ruault M-C, Carbonnel F. Animal Protein Intake and Risk of Inflammatory Bowel Disease: The E3N Prospective Study. Official journal of the American College of Gastroenterology | ACG. 2010;105(10).

37. Jowett SL, Seal CJ, Pearce MS, Phillips E, Gregory W, Barton JR, et al. Influence of dietary factors on the clinical course of ulcerative colitis: a prospective cohort study. Gut. 2004;53(10):1479.

38. Lees CW, Gros B, Kyle JA, Plevris N, Derikx L, Constantine-Cooke N, et al. 477c HABITUAL MEAT INTAKE IS ASSOCIATED WITH INCREASED RISK OF DISEASE FLARE IN ULCERATIVE COLITIS: INITIAL RESULTS FROM THE PREDICCT STUDY. Gastroenterology. 2023;164(6):S-1571.

39. Jadhav A, Bajaj A, Xiao Y, Markandey M, Ahuja V, Kashyap PC. Role of Diet-Microbiome Interaction in Gastrointestinal Disorders and Strategies to Modulate Them with Microbiome-Targeted Therapies. Annu Rev Nutr. 2023;43:355-383.

40. Bibi S, De Sousa Moraes LF, Lebow N, Zhu M-J. Dietary Green Pea Protects against DSS-Induced Colitis in Mice Challenged with High-Fat Diet. Nutrients. 2017;9(5).

41. Ahn E, Jeong H, Kim E. Differential effects of various dietary proteins on dextran sulfate sodium-induced colitis in mice. Nutr Res Pract. 2022;16(6):700-15.

42. Chiang JYL, Ferrell JM. Bile Acids as Metabolic Regulators and Nutrient Sensors. Annu Rev Nutr. 2019;39:175-200.

43. Kubota H, Ishizawa M, Kodama M, Nagase Y, Kato S, Makishima M, et al. Vitamin D Receptor Mediates Attenuating Effect of Lithocholic Acid on Dextran Sulfate Sodium Induced Colitis in Mice. International Journal of Molecular Sciences. 2023;24(4).

24

682   44.   Abdel-Razek EA-N, Mahmoud HM, Azouz AA. Management of ulcerative colitis by
683   dichloroacetate: Impact on NFATC1/NLRP3/IL1B signaling based on bioinformatics analysis
684   combined with in vivo experimental verification. Inflammopharmacology. 2024;32(1):667-82.
685   45.   Wolter M, Grant ET, Boudaud M, Pudlo NA, Pereira GV, Eaton KA, et al. Diet-driven
686   differential response of Akkermansia muciniphila modulates pathogen susceptibility. Molecular
687   Systems Biology. 2024;20(6):596-625-.
688   46.   Larabi AB, Masson HLP, Bäumler AJ. Bile acids as modulators of gut microbiota
689   composition and function. Gut Microbes. 2023;15(1):2172671.
690   47.   van Best N, Rolle-Kampczyk U, Schaap FG, Basic M, Olde Damink SWM, Bleich A, et
691   al. Bile acids drive the newborn's gut microbiota maturation. Nature Communications.
692   2020;11(1):3692.
693   48.   Islam KBMS, Fukiya S, Hagio M, Fujii N, Ishizuka S, Ooka T, et al. Bile Acid Is a Host
694   Factor That Regulates the Composition of the Cecal Microbiota in Rats. Gastroenterology.
695   2011;141(5):1773-81.
696   49.   Tian YA-O, Gui W, Koo IA-O, Smith PB, Allman EA-O, Nichols RG, et al. The
697   microbiome modulating activity of bile acids. Gut Microbes. 2020(Mar 5;11(4):979–996.).
698   50.   Bretin A, Zou J, San Yeoh B, Ngo VL, Winer S, Winer DA, et al. Psyllium Fiber Protects
699   Against Colitis Via Activation of Bile Acid Sensor Farnesoid X Receptor. Cellular and Molecular
700   Gastroenterology and Hepatology. 2023;15(6):1421-42.
701   51.   Sartor RB. Mechanisms of Disease: pathogenesis of Crohn's disease and ulcerative
702   colitis. Nature Clinical Practice Gastroenterology & Hepatology. 2006;3(7):390-407.
703   52.   Yang C, Merlin D. Unveiling Colitis: A Journey through the Dextran Sodium Sulfate-
704   induced Model. Inflammatory Bowel Diseases. 2024;30(5):844-53.
705   53.   Faith JJ, Ahern PP, Ridaura VK, Cheng J, Gordon JI. Identifying Gut Microbe–Host
706   Phenotype Relationships Using Combinatorial Communities in Gnotobiotic Mice. Science
707   Translational Medicine. 2014;6(220):220ra11-ra11.
708   54.   Darfeuille-Michaud A, Neut C, Barnich N, Lederman E, Di Martino P, Desreumaux P, et
709   al. Presence of adherent Escherichia coli strains in ileal mucosa of patients with Crohn's
710   disease. Gastroenterology. 1998;115(6):1405-13.
711   55.   Eun CS, Mishima Y, Wohlgemuth S, Liu B, Bower M, Carroll IM, et al. Induction of
712   bacterial antigen-specific colitis by a simplified human microbiota consortium in gnotobiotic
713   interleukin-10-/- mice. Infect Immun. 2014;82(6):2239-46.
714   56.   Remke M, Groll T, Metzler T, Urbauer E, Kövilein J, Schnalzger T, et al.
715   Histomorphological scoring of murine colitis models: A practical guide for the evaluation of colitis
716   and colitis-associated cancer. Experimental and Molecular Pathology. 2024;140:104938.
717   57.   Rath HC, Herfarth HH, Ikeda JS, Grenther WB, Hamm TE, Jr., Balish E, et al. Normal
718   luminal bacteria, especially Bacteroides species, mediate chronic colitis, gastritis, and arthritis in
719   HLA-B27/human beta2 microglobulin transgenic rats. J Clin Invest. 1996;98(4):945-53.
720   58.   Chassaing B, Srinivasan G, Delgado MA, Young AN, Gewirtz AT, Vijay-Kumar M. Fecal
721   Lipocalin 2, a Sensitive and Broadly Dynamic Non-Invasive Biomarker for Intestinal
722   Inflammation. PLoS One. 2012;7(9):e44328.
723   59.   Bai JDK, Saha S, Wood MC, Chen B, Li J, Dow LE, et al. Serine Supports Epithelial and
724   Immune Cell Function in Colitis. The American Journal of Pathology. 2024;194(6):927-40.
725   60.   Derrien M, van Baarlen P, Hooiveld G, Norin E, Muller M, de Vos W. Modulation of
726   Mucosal Immune Response, Tolerance, and Proliferation in Mice Colonized by the Mucin-
727   Degrader Akkermansia muciniphila. Front Microbiol. 2011;2.
728   61.   Chetnik K, Benedetti E, Gomari DP, Schweickart A, Batra R, Buyukozkan M, et al.
729   maplet: an extensible R toolbox for modular and reproducible metabolomics pipelines.
730   Bioinformatics. 2022;38(4):1168-70.
731
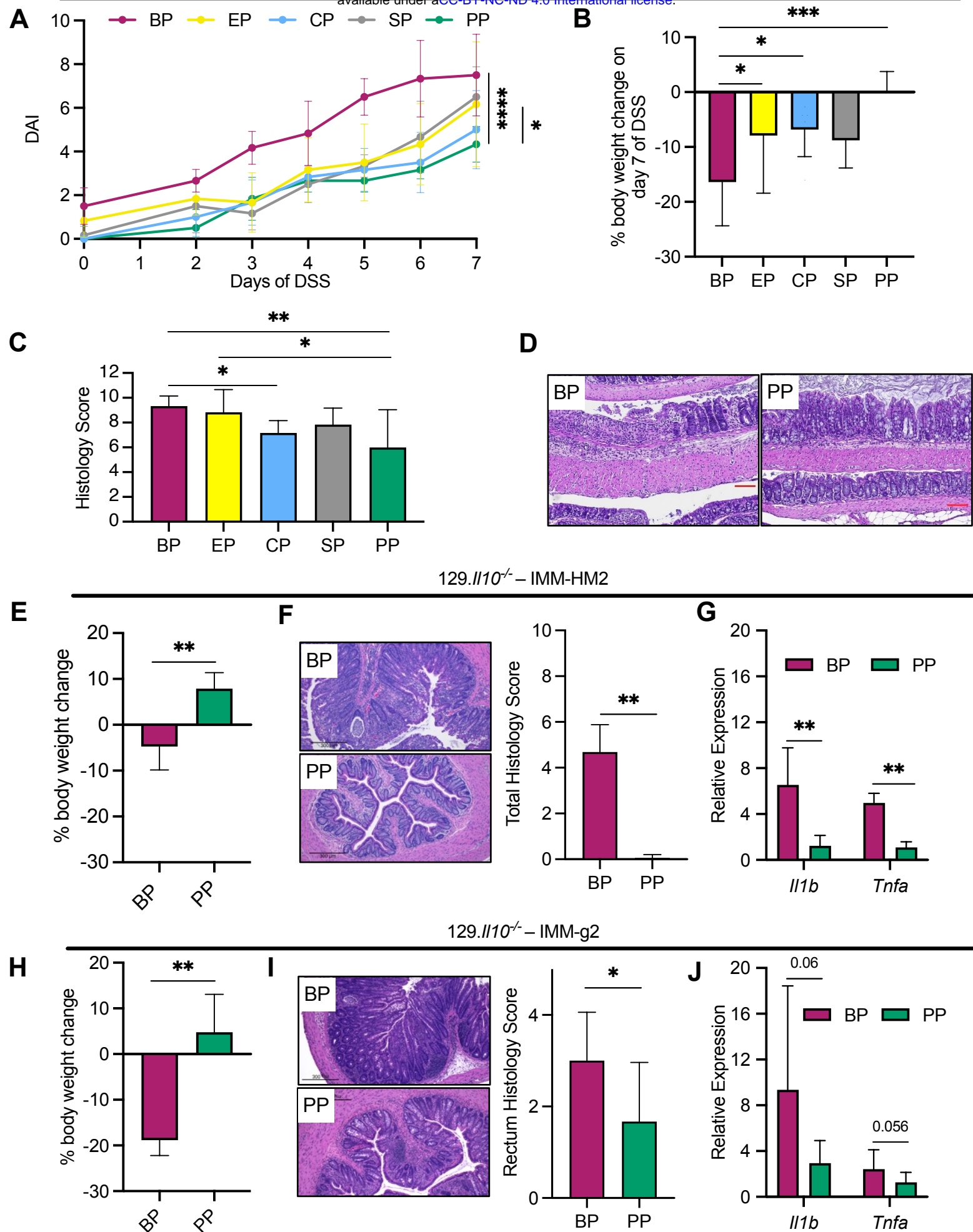
Figure 1
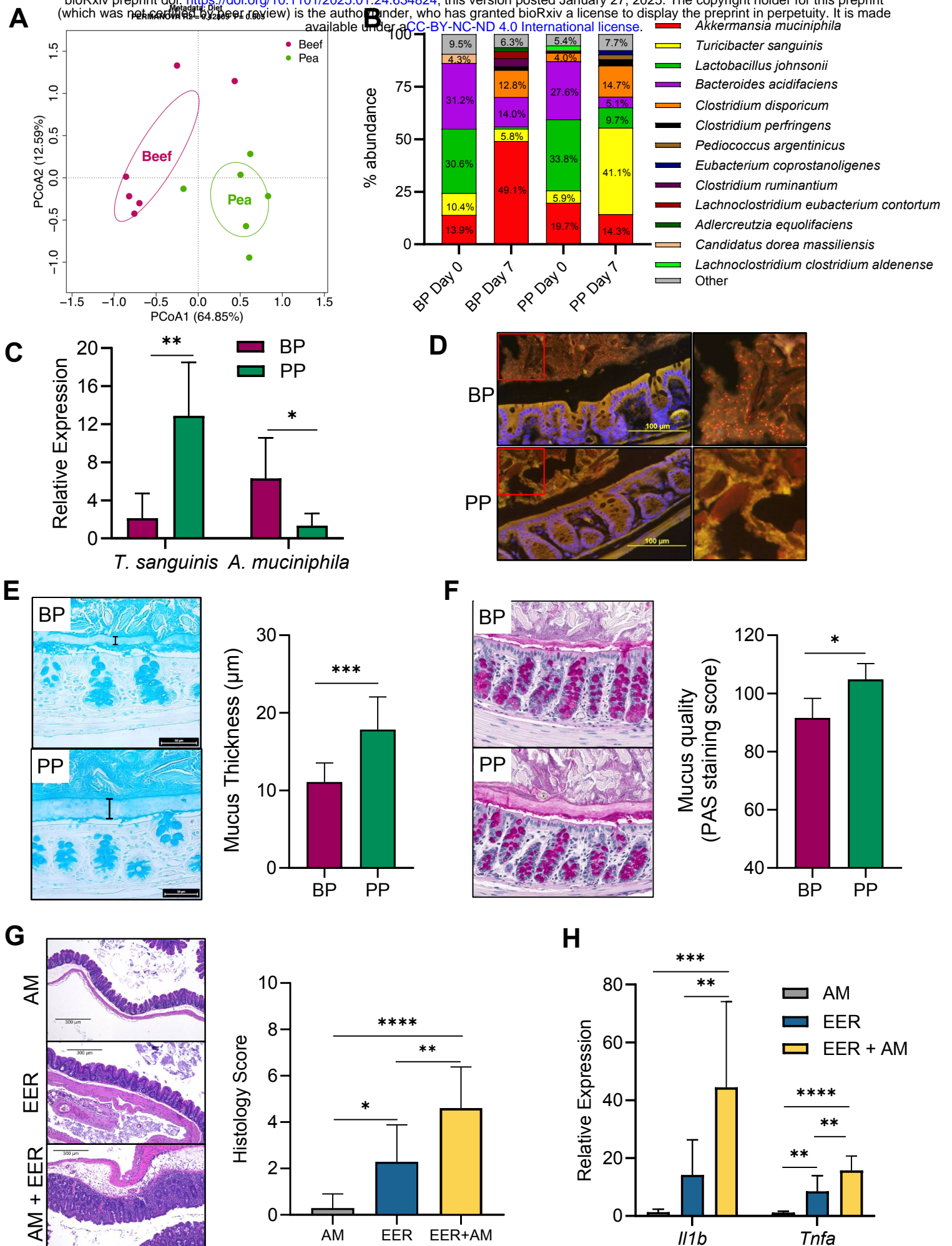
Figure 2
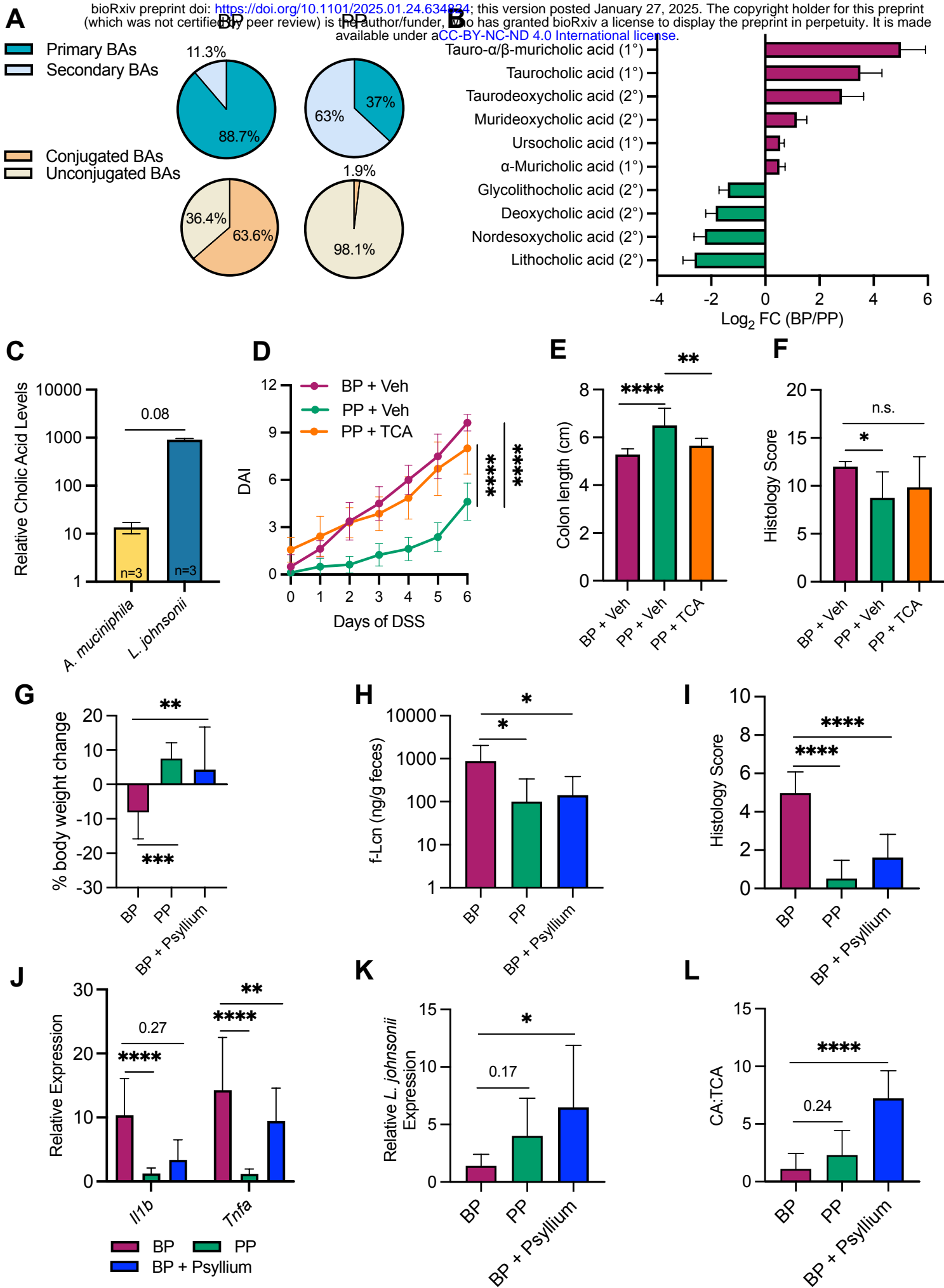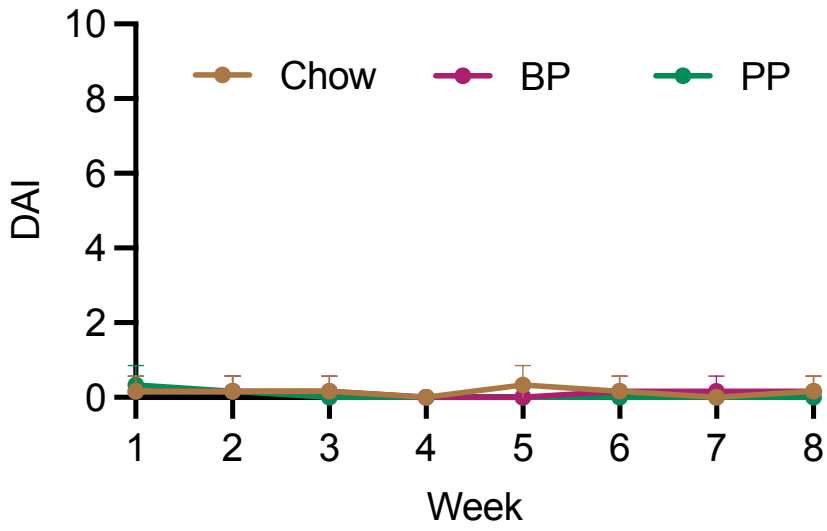
Figure 3

Figure 4

A

B
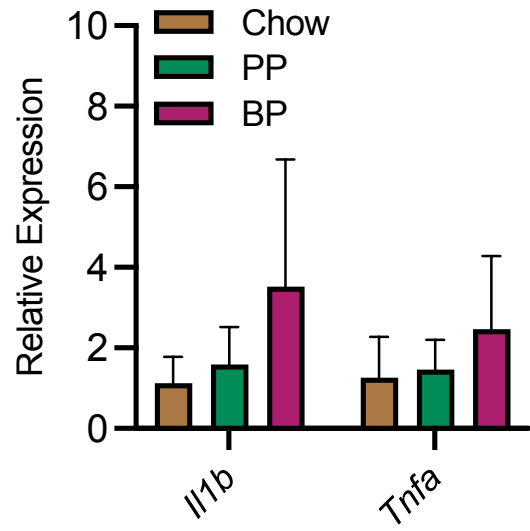
Figure S1

A

Legend:
- *Akkermansia muciniphila* (red)
- *Turicibacter sanguinis* (green)
- *Bacteroides acidifaciens* (orange)
- *Clostridium disporicum* (yellow)
- *Lactobacillus johnsonii* (blue)
- Other (gray)

Beef Day 0 — Relative Abundance (0–100), samples B-1 through B-6

Pea Day 0 — Relative Abundance (0–100), samples P-1 through P-6

B

Legend:
- *Akkermansia muciniphila* (red)
- *Turicibacter sanguinis* (green)
- *Bacteroides acidifaciens* (orange)
- *Clostridium disporicum* (yellow)
- *Lactobacillus johnsonii* (blue)
- Other (gray)

Beef Day 7 — Relative Abundance (0–100), samples B-1 through B-6

Pea Day 7 — Relative Abundance (0–100), samples P-1 through P-6

Figure S2

A

B

Figure S3

A

	H&E	MALDI
Vehicle		
TCA		

B
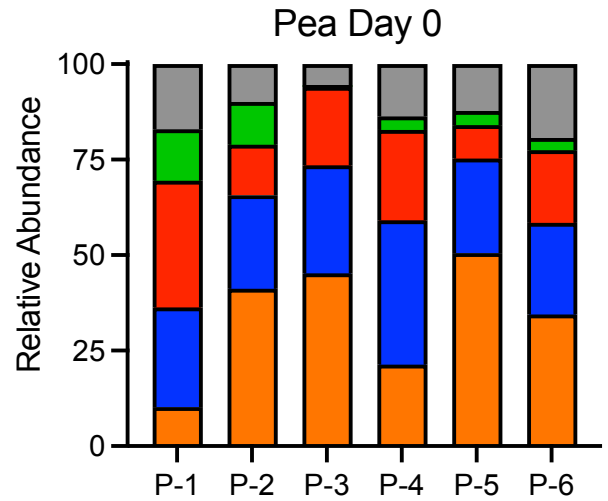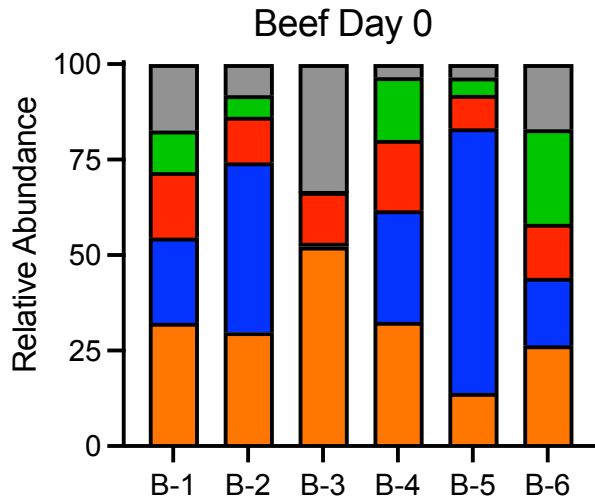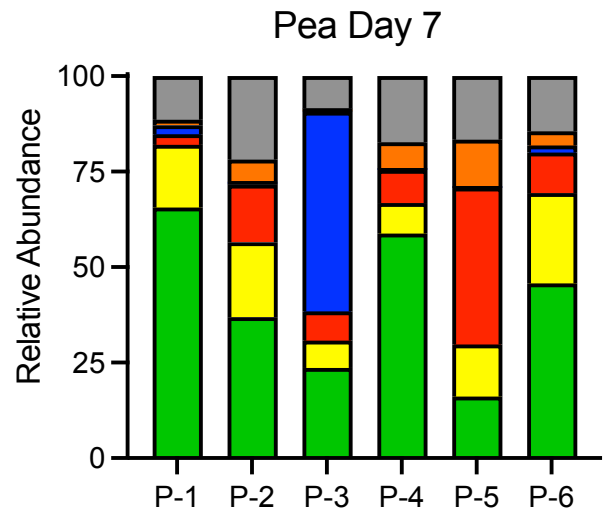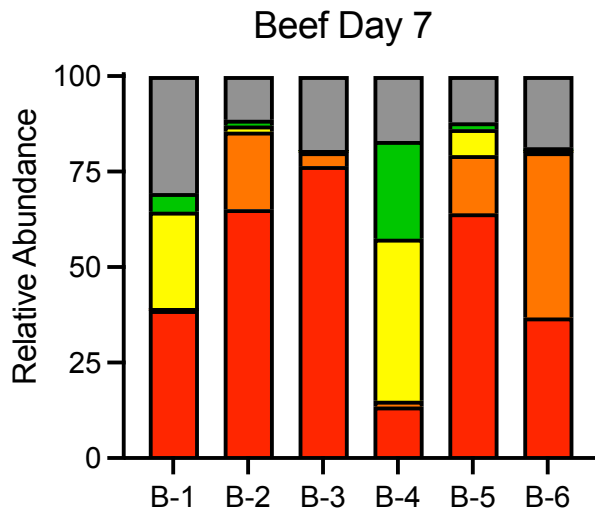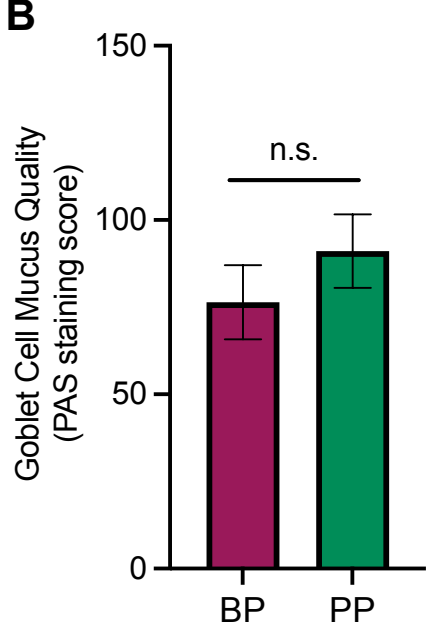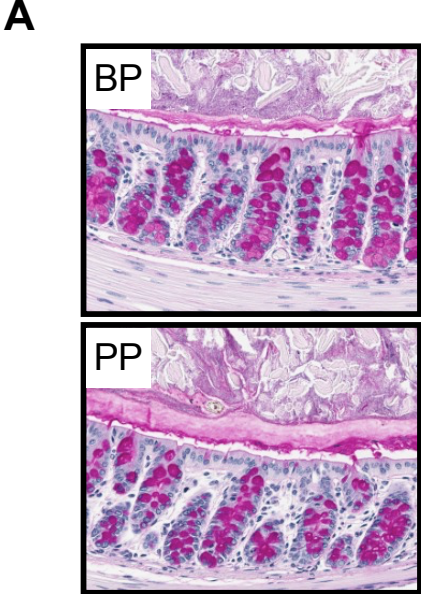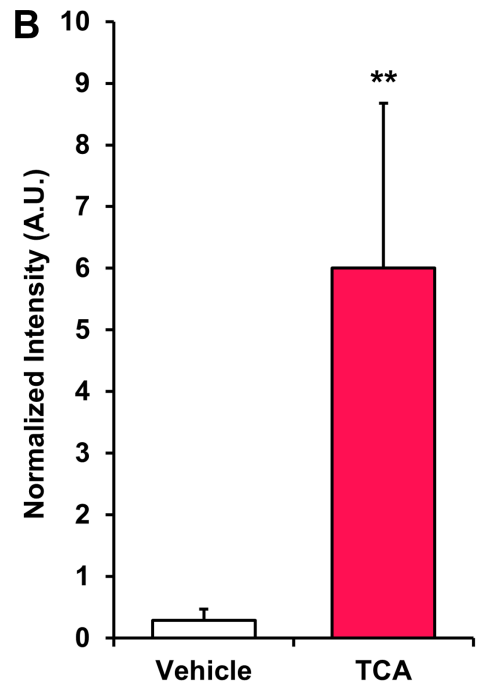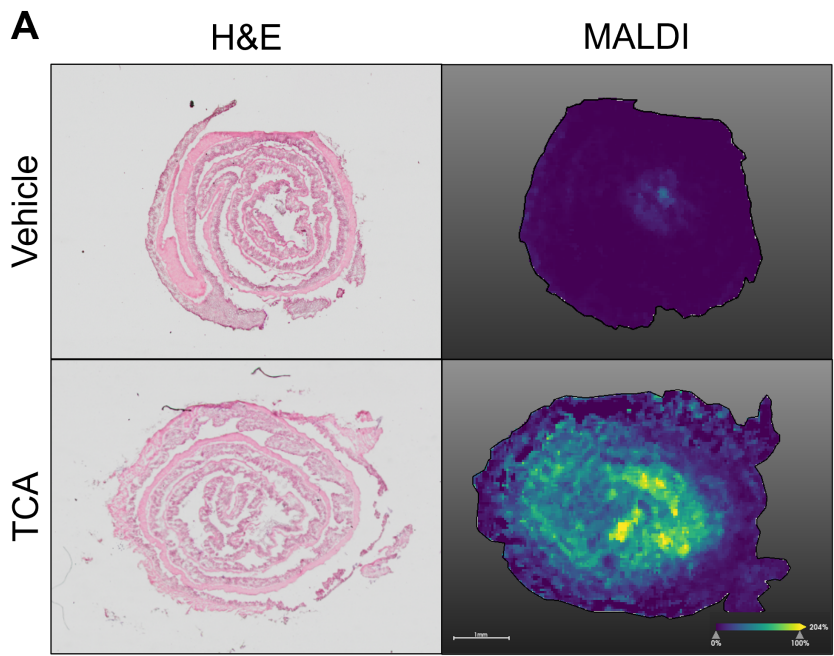
Figure S4

A
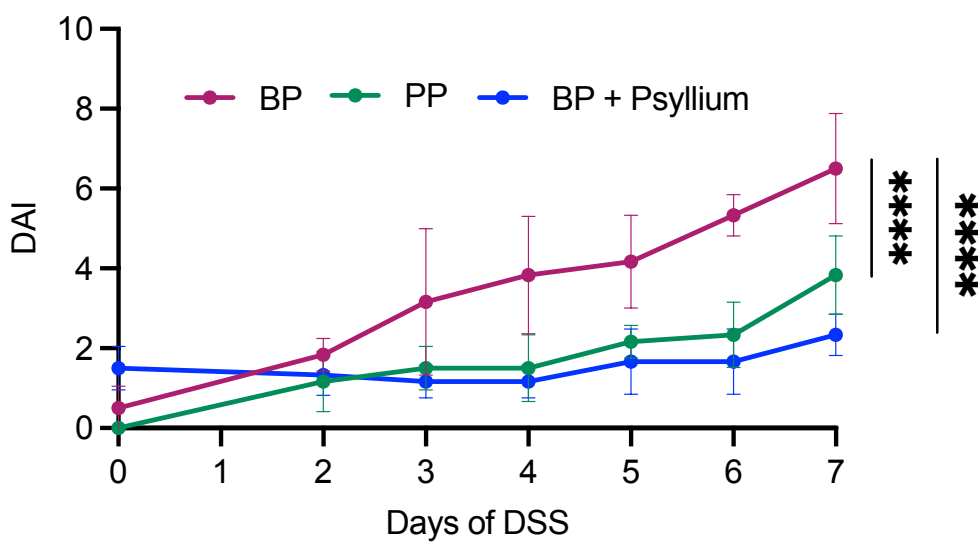
B
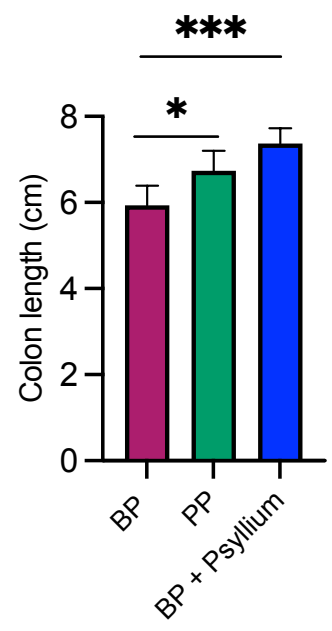
Figure S5

Table S1. Experimental Diet Formulations

Ingredient	Beef	Casein	Egg	Pea	Soy	Beef + Psyllium
	gm	gm	gm	gm	gm	gm
Casein	0	200	0	0	0	0
Soy Protein, Supro 661	0	0	0	0	202.3	0
Egg Whites	0	0	210.9	0	0	0
Beef Protein Isolate, Sigma	226.9	0	0	0	0	226.9
Pea Protein, Pure Bulk	0	0	0	209.1	0	0
L-Cystine	3	3	3	3	3	3
Corn Starch	398.486	397.486	389.286	398.486	395.486	385.329
Maltodextrin 10	132	132	132	132	132	132
Sucrose	100	100	100	100	100	100
Psyllium	0	0	0	0	0	52.63
Cellulose, BW200	50	50	50	50	50	0
Soybean Oil	70.8	70	70.2	51.8	63	70.8
t-Butylhydroquinone	0.014	0.014	0.014	0.014	0.014	0.014
Mineral Mix S10022G	0	0	0	0	0	0
Mineral Mix S10001A	17.5	17.5	17.5	17.5	17.5	17.5
Calcium Phosphate, Dibasic	17.5	17.5	17.5	17.5	17.5	17.5
Calcium Carbonate	0	0	0	0	0	0
Potassium Citrate, Monohydrate	0	0	0	0	0	0
Potassium Phosphate, Monobasic	0	0	0	0	0	0
Sodium Chloride	0	20.2	12.9	19.3	19.2	0
Vitamin Mix V10037	0	0	0	0	0	0
Vitamin Mix V10001	10	10	10	10	10	10
Biotin, 0.1%	0	0	0.4	0	0	0
Choline Bitartrate	2.5	2.5	2.5	2.5	2.5	2.5
Total	**1028.7**	**1020.2**	**1016.2**	**1011.2**	**1012.5**	**1018.2**
Protein (gm)	177.0	177.0	177.0	177.0	177.0	177.0
Carbohydrate (gm)	640.5	640.5	640.5	640.5	640.5	640.5
Fat (gm)	71.0	71.0	71.0	71.0	71.0	71.0
Fiber (gm)	50.0	50.0	50.0	50.0	50.0	52.63
Protein (kcal)	708.1	708.0	708.0	707.9	707.9	708.1
Carbohydrate (kcal)	2561.9	2561.9	2561.9	2561.9	2561.8	2561.9
Fat (kcal)	639.2	638.6	639.4	639.3	639.3	639.2
Total	3909.3	3908.6	3909.3	3909.2	3909.0	3909.3
Protein (gm%)	17.2	17.3	17.4	17.5	17.5	17.2
Carbohydrate (gm%)	62.3	62.8	63.0	63.3	63.3	63.0
Fat (gm%)	6.9	7.0	7.0	7.0	7.0	6.9
Protein (kcal%)	18.1	18.1	18.1	18.1	18.1	18.1
Carbohydrate (kcal%)	65.5	65.5	65.5	65.5	65.5	65.5
Fat (kcal%)	16.4	16.3	16.4	16.4	16.4	16.4
Sodium (g/kg)	8.8	8.8	8.8	8.8	8.8	8.8
kcal/gm	3.8	3.8	3.8	3.9	3.9	3.8

Table S2. Primer Sequences

Murine Targets		
Gene	Type	Sequence (5'-3')
B-actin	Forward	GGCTGTATTCCCCTCCATCG
	Reverse	CCAGTTGGTAACAATGCCATGT
Il1b	Forward	TGGGCCTCAAAGGAAAGAAT
	Reverse	CAGGCTTGTGCTCTGCTTGT
Tnfa	Forward	ACCCTCACACTCAGATCATCTTCTC
	Reverse	TGAGATCCATGCCGTTGG
Bacterial PCR Targets		
Akkermansia muciniphila	Akk-16S-F	GATAGTACCACAAGAGGAAGAGACG
	Akk-16S-R	TTCCCCCTCCATTACTCTAGTCTC
Lactobacillus johnsonii	Ljohn-16S-F	GCCTAGATGATTTTAGTGCTTGCAC
	Ljohn-16S-R	AGCAGAACCATCTTTCAAACTCTAGA
Turicibacter sanguinis	Turi-16S-F	TGTGACGGTACCTTATGAGAAAGC
	Turi-16S-R	GTTGACCAGTTTCCAATGACCCTC
Universal 16s Primer	Forward	ACTCCTACGGGAGGCAGCAG
	Reverse	ATTACCGCGGCTGCTGG
To amplify EER	Forward	U341F 5'-CCTACGGGRSGCAGCAG-3'
	Reverse	UA1406R 5'-ACGGGCGGTGWGTRCAA-3'